ELSEVIER

Catalysis Today 43 (1998) 69–77

CATALYSIS TODAY

Study of pillar precursors [Ga(III)–Al(III), Ln(III)–Al(III), Zr(IV)] for hydrothermally stable pillared clays

J.M. Domínguez[a,*], J.C. Botello-Pozos[b], A. López-Ortega[a], M.T. Ramírez[c], G. Sandoval-Flores[a], A. Rojas-Hernández[c]

[a]*Instituto Mexicano del Petróleo, STI, Gcia. Catalizadores, P.O. Box 14-805, 07730, Mexico, D.F., Mexico*
[b]*UNAM-FES-C, Secc. Química Analítica Cuautitlán-Izcalli, Mexico, D.F., Mexico*
[c]*UAM-I Dept. Química, Edif. R, Mexico, D.F., Mexico*

Abstract

The hydrolysis of mixed solutions of Al(III), Ga(III), Al(III), Ln(III) and Zr(IV) was studied by potentiometric, spectrophotometric and ^{27}Al- and ^{71}Ga-NMR techniques. For the Al–Ga system formation of $GaAl_{12}(OH)_{28}^{11+}$ species seems more probable into the pH range $4 \leq pH \leq 5$. Afterwards, the $Al_{13}(OH)_{32}^{7+}$ species predominate in agreement with thermodynamic data obtained by SUPERQUAD program. Both tetrahedral Ga^{IV} and Al^{IV} may coexist in solution, the interval being defined by potentiometric methods. For the Ln(III)–Al(III) systems ^{27}Al-and ^{139}La-NMR does not confirm the chemical interaction between the two species in solution, but the physicochemical properties of the La–Al/PILCS were different than Al/PILCS, suggesting a strong interaction in the solid state. Ce(III) and Ce(IV) ions do interact with Al(III) in solution, into the pH range $2.78 < pH < 3.99$, according with the spectrophotometric behavior. Finally, the Zr(IV) hydrolysis was followed by UV in the pH range greater than 2.0, showing the formation of $Zr_4(OH)_8^{8+}$ species, which was verified by calculations using SQUAD program, but the precipitation occurs at pH>3.0.

Keywords: Ga(III)–Al(III) pillar precursors; Ln(III)–Al(III) pillar precursors; Zr(IV) pillar precursor

1. Introduction

The insertion of polyoxocationic species into the interlamellar space of layered materials has been a subject of research in view of potential applications for the preparation of microporous materials used in separation technology and catalysis [1–3]. However, excepting the aluminum studies on the species formation, very little is known on the hydrolysis mechanisms of other inorganic polymer precursors or the influence of pH and cation concentration on the intermediate species formation [4]. Recently, the synthesis of aqueous $GaO_4Ga_{12}(OH)_{24}(H_2O)_{12}^{7+}$ and $GaO_4Al_{12}(OH)_{24}(H_2O)_{12}^{7+}$ polyoxocations was investigated [4,5] and these species were found isostructural with $Al_{13}O_4(OH)_{24}(H_2O)_{12}^{7+}$, which were synthesized previously by hydrolysis of Al(III) solutions [6]. However, these studies do not include the influence of the total metal concentration on the polynuclear species formation. The Ga(III) and Ga(III)–Al(III) polynuclear species are of interest for several reasons: the isoelectronic configuration that exists between Ga and Al and the larger ionic radius of

*Corresponding author. Fax: +525 5 5672927; e-mail: jmde@ec5500.sgia.imp.mx

0920-5861/98/$32.00
PII S0920-5861(98)00135-7

Ga(III), i.e. $r_{Ga(III)}$=0.62 Å vs. $r_{Al(III)}$=0.50 Å, would result in a larger polyoxocation with a thermally stable structure. The typical structure of these species is the well known modified Keggin ion configuration, having a central tetrahedrally coordinated species Ga(III) or Al(III) species, i.e. Al_{Td}(III), surrounded by twelve edge-linked octahedral Ga(III) or Al(III) species (Ga_{Oh}(III) or Al_{Oh}(III)). On the other hand, Ln(III)–Al(III) polynuclear species in solution have not been reported so far, but these systems are of interest because the possible stabilizing properties induced by Ln(III) polyvalent cations in the spinel-like structure of the interlamellar pillars. Also, the inherent catalytic properties of the Ln(III) may lead to unexpected results from the catalysis point of view.

In turn, Zr(IV) speciation studies have been rarely reported, which is due in part to the instability of their inorganic species in solution and the appearance of ageing effects [7,8]. Therefore, the purpose of the present work was twofold, firstly, to carry out a speciation study of the Ga(III)–Al(IIII), Ln(III)–Al(III) and Zr(IV) systems in solution, in order to determine the pH intervals and the influence of metal concentrations on the formation of species and secondly, to use the proper conditions derived from the previous study to prepare intercalated clays, which could have improved hydrothermal resistance properties that could be of interest for their use as catalysts supports in hydrocarbon hydrotreatment [3]. To this end, a combination of potentiometric and spectrophotometric analysis, ^{27}Al-, ^{139}La-, ^{71}Ga-NMR and equilibrium calculations using SUPERQUAD and SQUAD programs [9] were applied with the aim of determining the formation interval for the $Ga_pAl_q(OH)_r^{3p+3q-r}$, $Ln_pAl_q(OH)_r^{3p+3q-r}$, $Zr_p(OH)_r^{3p}$ polyoxocations and the alternate species that might coexist in solution.

A further verification of the chainlength was made by measuring the interplanar distance of the intercalates, using X-ray methods. Also, the polynuclear species formed in solution were used for intercalation of layered clays, with the purpose of improving their hydrothermal resistance properties. The textural and structural variations of the intercalated clays (Al–Ga, Al–Ln, Zr) were tested for their hydrothermal stability. In turn, these intercalates were evaluated as catalysts supports for hydrocarbons hydrotreatment [2,10].

2. Experimental methods

2.1. Potentiometric studies

Al(III), Ga(III) and Al(III)/Ga(III) solutions (with a concentration ratio Al/Ga equal to 12) were prepared from $Al(NO_3)_3{\cdot}9H_2O$ (Baker Analyzed, 99.1%) and $Ga(NO_3)_3{\cdot}9H_2O$ (Baker Analyzed, hp) in distilled/deionized and decarbonated water. The metal concentration of the stock solutions was determined by complexometry techniques. The Al(III) samples had a concentration range between 3.96 and 19.80 mol l^{-1} (10^{-3}), while the mixed Al–Ga solutions had concentrations from 3.96 and 19.80 mol l^{-1} (10^{-3}) of aluminum and 3.47–17.36 mol l^{-1} (10^{-4}) of gallium, respectively.

Three samples of each solution were titrated using NaOH (std.). The pH variations were monitored with a Tacussel-LPH430T pH-meter (ΔpH=0.001), fitted with a combined glass type electrode and internal reference, as well as a temperature probe. The temperature was controled with a MGW-Lauda T1 bath (ΔT=0.1°C) and the nitrogen stream was kept constant during the measurements. A previous correction for cell efficiency was applied before feeding data to the SUPERQUAD programs [9]. The pH was measured for all the hydrolyzed solutions accordingly with Tables 1–3, respectively. The potentiometric data allowed the determination of the $-\log \beta^*$ values, which corresponded to the formation constants, considering water and protons for equilibrium balance as recommended by IUPAC.

Table 1
The best models refined for Al(III) and Ga(III) hydrolysis by SUPERQUAD methods

Solutions	Species	$-\log \beta^* \pm \sigma$
Al(III)	$Al(OH)^{2+}$	5.29±0.04
	$Al_3(OH)_4^{5+}$	13.57±0.05
	$Al_{13}(OH)_{32}^{7+}$	110.54±0.10
Ga(III)	$Ga(OH)_2^+$	7.7±0.03
	$Ga(OH)_3$	10.71±0.01
Al(III) and Ga(III)	$Al(OH)^{2+}$	5.37±0.13
	$Al_3(OH)_4^{5+}$	13.23±0.05
	$Al_{13}(OH)_{32}^{7+}$	110.27±0.10
	$Ga(OH)_3$	10.13±0.01
	$Al_{12}Ga(OH)_{28}^{11+}$	89.40±0.17

Table 2
Ga(III)–H_2O systems for NMR studies

System	OH/M ratio	pH
A	0.00	2.655
B	0.30	3.096
C	0.50	3.248
D	1.50	3.718
E	2.30	4.224

Table 3
Al(III)–Ga(III)–H_2O systems for NMR studies

System	OH/M ratio	pH
A	0.00	2.781
B	0.22	3.119
C	0.31	3.359
D	0.40	3.547
E	0.54	3.782
F	1.54	4.053
G	2.31	4.295

Similarly, the mixed Al–Ln (La, Ce) species were synthesized from $AlCl_3{\cdot}6H_2O$ (6.13 M Al) and $Ln(NO_3)_3$ (433.02 g/gmol of La, 434.23 g/gmol of Ce) solutions at pH's between 3 and 3.5, at 60°C, with Ln/Al ratios: 0.0081, 0.0163, 0.0326, 0.0652 and 0.1304. 1 M. A HCl solution was used for pH control under stirring.

The Zr(IV) solutions were prepared from the slow hydrolysis of $ZrCl_4$ solutions (1×10^{-4} M) using NaOH (std.), and this was followed by potentiometric and UV spectroscopy methods. The Zr(IV) system was studied before by C.F. Baes and Hannane et al. [7,8], who used a methodology based upon extraction with several solvents in concentrated acidic solutions and the Zr complexes in solution were aged before the measurements. The second author used Raman spectroscopy. In contrast, in the present work, a spectrophotometric method was applied to determine the equilibrium constants. A series of fresh solutions were used to this end and the measurements were performed in stationary state at different time intervals. The Zr(IV) solutions were prepared using decarbonated water at several concentrations. The hydrolysis was monitored by potentiometric methods and by UV spectrophotometry, at distinct pHs, up to the precipitation point. Both temperature and surrounding environment were kept under control, i.e. T=25°C in a dynamical nitrogen atmosphere.

2.2. NMR studies

The ^{27}Al, ^{139}La and ^{71}Ga NMR spectra were obtained on a Bruker DMX-500 spectrometer at 25°C. $AlCl_3{\cdot}6H_2O$, $La(NO_3)_3$ and $Ga(H_2O)_6^{3+}$ were used as references, and D_2O was used for external field frequency lock. However, some of the cationic systems in solution were not well suited for NMR studies, i.e. Ce^{3+} and Zr^{4+}. In these cases a UV characterization was made using a PE-Lambda 18 spectrophotometer, fitted with a silica-gel-Beckman type cell.

2.3. Pillared clays preparation

The hydrolysis products were used for preparing pillared clays by means of the intercalation of the polyoxocationic species (i.e. in solution) into the interlamellar space of the layered materials. The pH was the critical parameter in each case, as follows:

1. –(Al–Ga)-PILCS were prepared from 130 g of purified Montmorillonite type clays from Oaxaca, Mexico, which were suspended in 150 ml of bidistilled water and 3 ml HCl (1 M) were added for pH adjustments. The (Al+Ga) aqueous solutions (Ga/La≅1) with OH/M ratios of about 2.0 were stirred at room temperature and the clay suspension was added slowly, under pH conditions in the interval $3.9\leq pH\leq 4.0$. After centrifugation (1×10^3 rpm) and drying at 40°C in air, the solids were calcined at 400°C (2 h), then were studied by X-ray diffraction in order to measure the interplanar distances (d).
2. –(Al–Ln)-PILCS were prepared from a clay-water (bidistilled) suspension (40% w/v), which was saturated with NaCl (0.1 M) in order to produce a homoionic clay (i.e. 5 meq Na^+/g_{clay}). The precursor (Al–Ln) solution was prepared by hydrolysis of $AlCl_3/Ln(NO_3)_3$ salts with 750 ml of a 1 M solution of NaOH, until a OH/M ratio equal to 2 was reached. Then, 2 meq [Al–Ln]/g_{clay} was added to the clay suspension at 50°C, under moderate stirring (24 h), always keeping pH around 3.7. After washing with demineralized water and centrifugation, the solids were dried at room tempera-

ture under air flow, then were calcined at 400°C (2 h).

3. The Zr-PILCS were prepared from a 1 M $ZrCl_4$ hydrolyzed solution (with a std. 1 M NaOH solution at room temperature) which was kept under moderate stirring in nitrogen atmosphere. Each point was left to reach equilibrium before the next addition. The final point of the hydrolysis was marked by a pH value of about 1.8–2.0, just at the starting point of the Zr ion precipitation. After heating at 50°C (3 h) the mixture was cooled down to room temperature, then it was washed, centrifugated and dried at 25°C, before calcination at 400°C (2 h).

3. Results

3.1. Potentiometric studies

The mean titration curves for Al(III), Ga(III) and Al(III)/Ga(III) solutions are shown in Fig. 1(a)–(c) for the region of interest. In all cases an increase of pH proceeds until a molar ratio OH/M(III)=2. The potentiometric data were feed to SUPERQUAD programs [9] for equilibrium constants refining. The best fits corresponded to the model shown in Table 1.

The species and equilibrium constants in Table 1 are very similar to those obtained by Brown et al. [6], but the heteropolynuclear complex $Al_{12}Ga(OH)_{28}^{11+}$ has been recently confirmed by Botello et al. [12] with the aid of ^{71}Ga-NMR as shown in Fig. 1(d). The distribution diagram of Ga(III) species, which was built using the data reported in Table 1 for this particular system, which explains this behavior.

The model obtained in this work for Al(III) hydrolysis is similar to the models proposed by Brown et al. [6] and Öhman et al. [11], who considered a polynuclear species for aluminum, i.e. $(Al_{13}(OH)_{32}^{7+})$ having a Keggin ion type structure.

The species distribution diagram for the Al(III)–Ga(III) system is displayed in Fig. 1(e), for a specific concentration, i.e. $[Al(III)]_{tot}=19.80\times10^{-3}$ M, $[Ga(III)]_{tot}=17.36\times10^{-4}$ M. Here the tridecamer, i.e. $Al_{12}Ga[OH]_{28}^{11+}$, appears clearly in the pH interval 3.9<pH<5.0.

The $AlCl_3$–$La(NO_3)_3$ and $AlCl_3$–$Ce(NO_3)_3$ solution series were evaluated by potentiometric methods and were characterized by means of UV spectroscopy, as indicated in Figs. 2–4. La(III) solutions presented two broad absorption maxima around 245 and 285 nm, with a profile similar to KNO_3 absorption spectrum (Fig. 2). This indicated a rather moderate $La(NO_3)_3$ hydrolysis, which is evidenced by the presence of NO_3^- anions free in solution. On the other hand, the pure Ce(III) hydrolysis gave rise to a broad absorption band, which was different than KNO_3 (Fig. 3). However, in the hydrolysis of the mixed Ce(III)–Al(III) solutions a UV-absorption profile similar to KNO_3 is observed again, confirming the previous results obtained with La(III) salts hydrolysis. In Fig. 4 the entire series of hydrolysis for Ce(III)–Al(III) is reported, observing the same UV-absorption profile, which is enhanced by the increasing pH, i.e. from bottom to top.

The study of Zirconium solutions by UV absorption techniques led to the results shown in Fig. 5, where the spectra look similar to those of Zr(IV) solutions (0.05 M) at distinct pH values. The absorption increases with the pH, thus indicating the hydrolysis progression in function of the NaOH content. The data for Zr solutions were feed to the SQUAD programs and the results were as follows: Species $Zr(OH)^{3+}$, $Zr(OH)_3^+$ and $Zr_4(OH)_8^{8+}$ have $-\log\beta$ values equal to -0.3, $+5.1$ and $+2.37$, respectively. From these results, a species distribution diagram was obtained (Fig. 6). It is clear that for 0.01 M concentrations the polynuclear species, i.e. Zirconium tetramer, predominates only in the pH range above 1.8. In this viewpoint, the pillaring of layered materials must be realized under pH values equal to 2.0 or higher. The interplanar distance of the Zr(IV)-pillared clays was equal to 19.8, before calcination, which indicated an expansion of about 5.4 Å, which might correspond to the insertion of 1 tetramer layer in the interlamellar space. Fig. 7 shows the absorption coefficients (i.e. SQUAD results). These results show clearly that the tetramer species predominate, their absorption coefficient being higher than mononuclear species.

3.2. Thermal properties of Ln(III)–Al(III)-Pillared clays (PILCS)

The variation of the X-ray basal peak areas provided information on the pillared-structure integrity, i.e. the peak profile indicates the structure stability in function

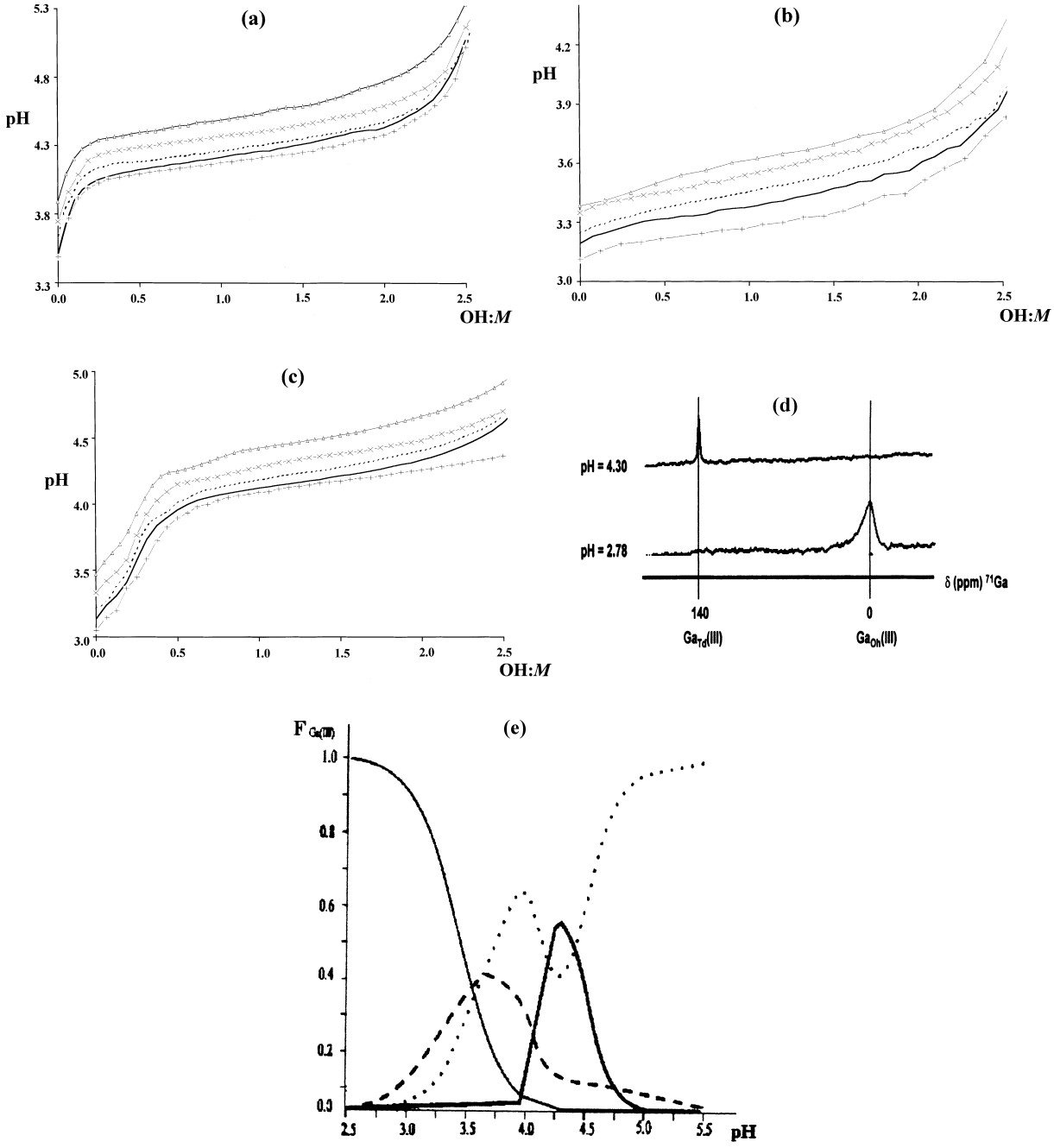

Fig. 1. (a) Titration curves for Al(III) at 25°C: △△△ 3.96×10^{-3} M, xxx 7.92×10^{-3} M, - - - 11.88×10^{-3} M, ——— 15.84×10^{-3} M, +++ 19.80×10^{-3} M. (b) Titration curves for Ga(III) at 25°C: △△△ 3.33×10^{-4} M, xxx 6.66×10^{-4} M, - - - 9.99×10^{-4} M, ——— 13.33×10^{-3} M, +++ 16.66×10^{-4} M. (c) Titration curves for Al(III)-Ga(III) at 25°C: △△△ 3.96×10^{-3} M/3.47×10^{-4} M, xxx 7.92×10^{-3} M/6.94×10^{-4} M, - - - 11.88×10^{-3} M/10.42×10^{-4} M, ——— 15.84×10^{-3} M/13.89×10^{-4} M, +++ 19.80×10^{-3} M/17.36×10^{-4} M. (d) ^{71}Ga-NMR spectra for mixed Al(III)-Ga(III) aqueous solutions. The signal at 140 ppm confirms a Keggin ion structure for a tetrahedral Ga(III) surrounded by 12 octahedral Al(III). (e) Species distribution diagram for Ga(III) in solution. $[Al(III)]_{tot}=19.80\times10^{-3}$ M, $[Ga(III)]_{tot}=17.36\times10^{-4}$ M. _____ Ga(III), - - - - $Ga(OH)_2^+$, · · · · · · $Ga(OH)_3$, — $Al_{12}Ga(OH)_{28}^{11+}$.

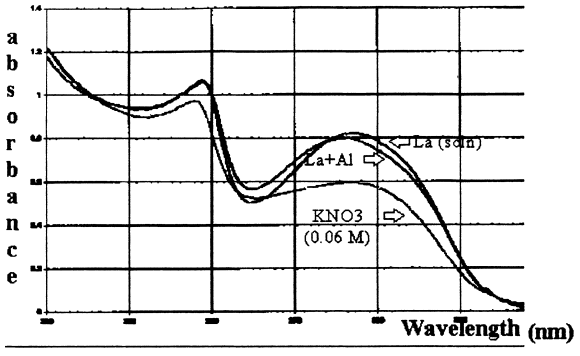

Fig. 2. UV spectra of La, La–Al, KNO_3 (0.06 M) species in solution.

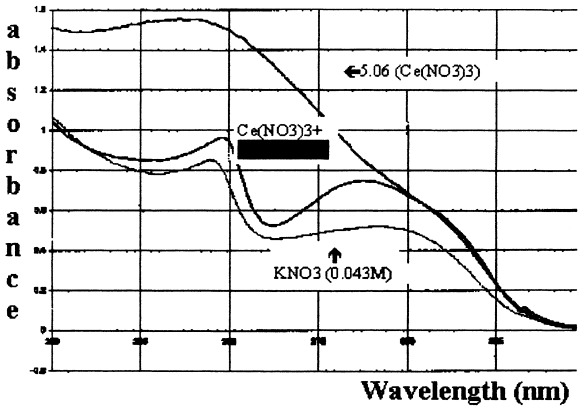

Fig. 3. UV spectra of $Ce(NO_3)_3$ −5.06 M, Ce(2.78 M)-Al and KNO_3 (0.0438 M).

Table 4
Structural stability variation (%) of the steamed Al/Ce PILCS with respect to temperature (in 100% vapor)

Temperature (°C)	% Variation of X-ray peak profile area
400	–
500	+98.1
600	+92.7
700	+37.4
800	−13.6

of the temperature under 100% H_2O vapor. Only the Ln(III)–Al(III) systems are described but the other cases were found similar. Table 4 describes the variation of the basal peak (0 0 1) areas in function of temperature, i.e. 400–800°C in 100% vapor. The peak areas increase with temperature up to about 98% at 500°C, then decrease down to −13.6% at 800°C.

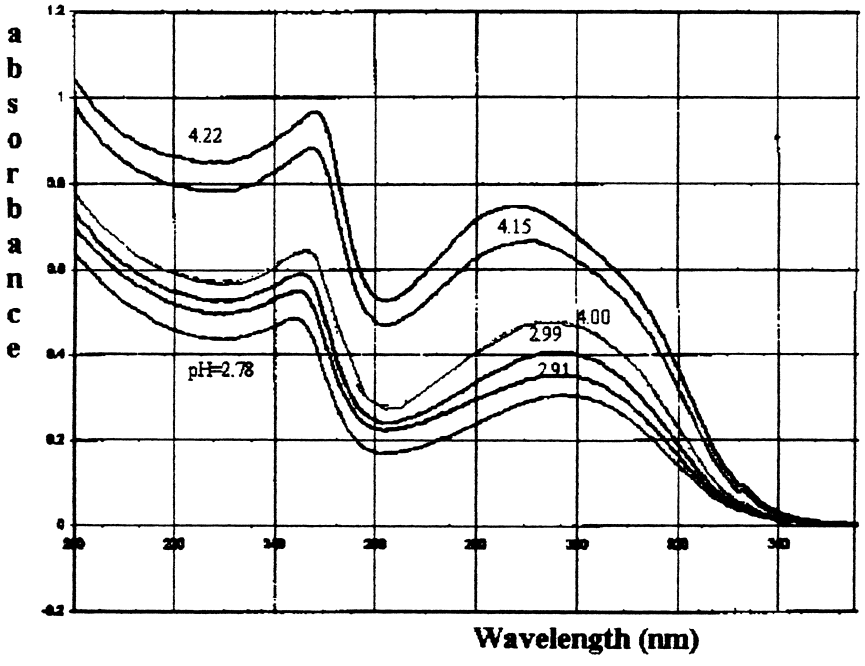

Fig. 4. UV spectra of Ce–Al hydrolysis series (pH decreasing from 4.22 to 2.78).

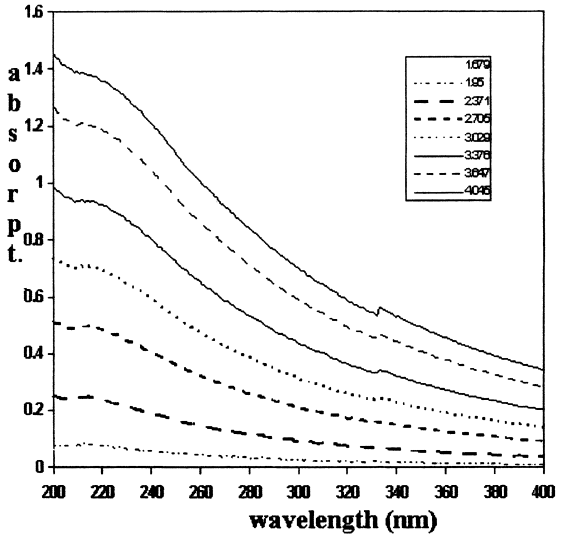

Fig. 5. UV absorption for the Zr solution series.

Similarly, Table 5 indicates the diffraction peak profile areas of the La(III)–Al(III) system in function of the treatment temperature (i.e. from 400 to 800°C, 100% H_2O vapor).

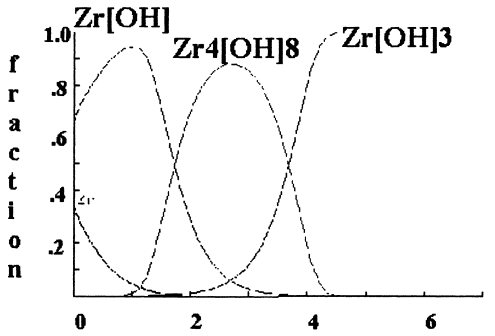

Fig. 6. Species distribution diagram for polyoxocations in aqueous solutions.

Table 5
Structural stability variation (%) of the steamed Al/La PILCS with respect to temperature (in 100% vapor)

Temperature (°C)	% Variation of X-ray peak profile area
400	–
500	+3
600	+15
700	−29
800	−55

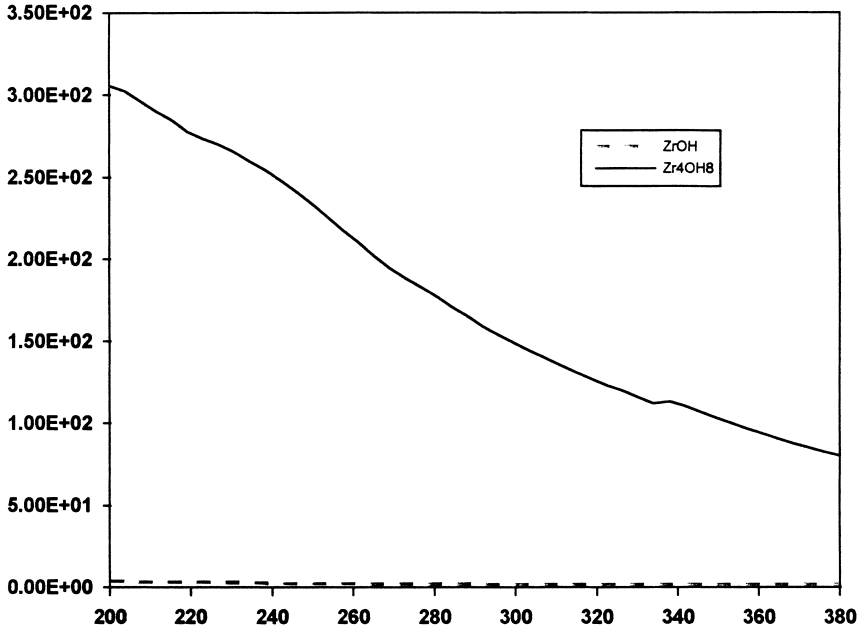

Fig. 7. Absorption coefficients for the tetramer species.

As observed, the Ce(III)–Al(III) is more stable than the La(III)–Al(III) system.

4. Discussion

The combination of potentiometric techniques and SUPERQUAD calculations, together with UV and NMR spectroscopies, allowed a study on the species formation in solution of the Al(III)–Ga(III), Al(III)–Ln(III) and Zr(IV) systems. In the former system the $GaAl_{12}(OH)_{28}^{11+}$ polyoxocation predominates in the interval 3.9<pH<5.0, for specific concentrations, i.e. $[Al(III)]_{tot}=19.8\times10^{-3}$ M, $[Ga(III)]=17.36\times10^{-4}$ M. At lower concentrations the pH interval becomes narrower than the previous one, i.e. 4.1<pH<4.7 for $[Al(III)]_{tot}=3.96\times10^{-3}$ M, $[Ga(III)]=3.47\times10^{-4}$ M. Also, the presence of $^{71}Ga^{IV}$ in a high molecular complex was confirmed by ^{71}Ga-NMR spectroscopy. The typical behavior showed that at low hydrolysis levels (OH/M=0–0.22) only octahedral gallium appears (Ga^{VI}) but at OH/M ratios of 0.31–0.40 the ^{71}Ga disappears, probably due to a symmetry loss. At OH/M values equal to or higher than 0.54 the ^{71}Ga (at $\delta=139$ ppm, tetrahedral) signal appears clearly. The pillaring of layered clays with a mixed ($Ga_{Td}+Al_{Oh}$) polyoxocationic solution led to stable materials with a *d*-spacing of about 20.5 Å.

For the Ln(III)-Al(III) systems the potentiometric data obtained after NaOH titration were not suitable for the convergence of the equilibrium constants using the SUPERQUAD program. Instead of this, UV spectroscopy was applied in order to generate more reliable data, but the signals recorded were only assigned to the presence of NO_3^- anions in solution, i.e. a similar UV-absorption profile is compared positively against KNO_3 (Figs. 2–4), which indicated that only a slight interaction occurs in solution. The ^{27}Al-NMR spectra did not show either a variation of both Al_{Oh}-, Al_{Td}-NMR peaks, thus the chemical interaction of Al polyoxocations with the Lanthanides (La(III), Ce(III)) in aqueous solution was not confirmed. This is probably due to the distinct hydrolysis range of the individual salts, i.e. 2.8<pH<4.5 for $Al(NO_3)_3$ and about 8<pH<11 for $Ln(NO_3)_3$. However, when the polyoxocationic solutions containing the Ln(III)–Al(III) mixed species are used in the pillaring of layered clays, both structural and hydrothermal resistance of the Ln–Al/PILCS change dramatically. This indicates that, Ln(III) do interact with the Al(III) complexes upon calcination in air, leading to formation of very stable spinel-like structures. The X-ray diffraction profiles of the Ln(III)–Al(III)/PILCS shows higher *d*-spacings, i.e. up to 21 Å, as well as higher intensity and symmetry in the interval 400–600°C, i.e. up to about 98.1–92.7% peak area increase for Ce(III)–Al(III)/PILCS and +15% peak area variation for La(III)–Al(III)/PILCS. This structural reordering may arise from the hydrothermal conditions in which water vapor at high temperature (i.e. T>400°C) acts as a transport medium into the clay flakes, thus associating the pillaring material left outside the pillars into more regular intercalates. At temperatures higher than 600°C under 100% H_2O vapor, a clear structural degradation starts, leading to 29% XRD-peak area loss at 700°C and 55% loss at 800°C for La(III)–Al(III)/PILCS, but in the Ce(III)–Al(III)/PILCS system a gain of 37.4% still persists at 700°C and finally, a loss of only 13.6% occurs at 800°C. These results confirm previous reports [13,15], which disclose a series of pillared clays prepared by ion exchanging $CeCl_3$, $LaCl_3$ and $LiCl_3$ aqueous solutions with Na^+/Ca^{2+} Montmorillonite.

Previous analysis [14] by EELS (Electron Energy Loss Spectroscopy) of the calcined solids indicated that the EELS profile of the (La–Al)-Montmorillonite is different to the profile corresponding to the Al-Montmorillonite, which means that the chemical environment of both aluminum (Al(III)-L edges at 72 eV) and oxygen (O_k-edges at 531 eV) atoms associated with the pillar structure is indeed perturbed by the introduction of Ln cations, thus indicating the presence of rare-earth cations in the pillar structure of the PILCS [13,14].

The Zr(IV) complexes in solution were studied by potentiometric (coupled with Superquad calculations) methods and UV spectroscopy. Although, this is an unstable system which evolves with time, the equilibrium conditions were reached by means of the control of surrounding environment (i.e. under N_2 dynamical flow) and constant temperature (i.e. T=25°C) as well as by the use of decarbonated aqueous solutions under N_2 flow. The UV methods allowed us to obtain the raw data for assigning the more probable species in solution, but potentiometric determinations are also underway to confirm those

results. In the previous work reported by Baes [7] ageing of Zr(IV) solutions ($\ll$0.1 M) was performed before the potentiometric measurements, i.e. 60 days. In our case, the titration was made using fresh solutions only (0.1 M) and waiting for equilibration, i.e. about 7 h runs. Baes et al. did report mononuclear species ($Zr(OH)^{3+}$) formation and polynuclear $Zr_3(OH)_4^{8+}$, $Zr_3(OH)_5^{7+}$ and $Zr_4(OH)_8^{8+}$ species. In the present work, the trimeric species were not found, which could be explained in basis of the ageing treatment performed by Baes et al. Another difference is that those authors made several determinations for one single species at low concentrations (i.e.$\ll$0.1 M), arguing that higher concentrations caused some precipitation. In the present work, this point was not confirmed. More probably, the precipitation at higher Zr concentrations could be related with ageing. In the present work, the pH interval for $Zr_4(OH)_8^{8+}$ tetramers formation was established, i.e. 1.8< pH <3.7 (Fig. 6). In this respect, the species distribution diagram (Fig. 6) is similar to the one reported by Baes et al. [7].

5. Conclusions

The search of more stable intercalated layered materials was accomplished in this work by determining the conditions for species formation in solution. Four systems were monitored by potentiometric, UV and NMR methods: Ga(III)–Al(III), Ln(III)–Al(III), Zr(IV). In the former case polynuclear species form in the interval 3.9<pH<5.0 at concentrations $[Al(III)]_{tot}=19.8\times10^{-3}$ M, $[Ga(III)]=17.36\times10^{-4}$ M, but this pH range is narrowed for lower concentrations, i.e. 4.1<pH<4.7 for $[Al(III)]_{tot}=3.96\times10^{-3}$ M, $[Ga(III)]=3.47\times10^{-4}$ M. For the Ln(III)–Al(III) system the Ln–Al interaction in solution was elusive, but the hydrothermal properties of the clay intercalated materials indicate that, insertion of Ln(III) in the pillar structure may occur, which provokes a stacking reordering and further resistance at high temperature (800°C under 100% steam). This results confirm previous works [13–15], which have pointed out that intercalation of rare-earth cations like Lanthanum into the pillar structure of the layered materials improve their hydrothermal resistance.

Finally, the Zr(IV) hydrolysis study indicated the progressive formation of mononuclear and tetramer species, i.e. $Zr(OH)^{3+}$, $Zr(OH)_3^+$ and $Zr_4(OH)_8^{8+}$, the higher molecular weight species being predominant in the interval 1.8<pH<3.7. In turn, the use of those conditions led to intercalates with an interplanar spacing of 19.8 Å, that is a 5.4 Å chainlength, which is about the molecular diameter of a four-branched $Zr_4(OH)_8$ species.

Acknowledgements

This work was possible thanks to the Financial grant of IMP/PEMEX program No. FIES-96-31-III

References

[1] R.M. Barrer, Pure Appl. Chem. 61 (1989) 1903.
[2] M.E. Landis, B.A. Afdembrik, I.D. Johnson, G.W. Kiiker, M.K. Rubin, J. Am. Chem. Soc. 113 (1991) 3189.
[3] C.E. Ramos-Galván, J.M. Domínguez, G. Sandoval-Robles, A. Castillo-Mares, J. Appl. Catal. 150 (1997) 35–52.
[4] J.W. Akkit, J.M. Elders, L.R. Fountaine, AM. Kundo, J. Chem. Soc. Dalton Trans. (1989) 1887.
[5] S.M. Bradley, R.A. Kydd, R. Yamdagni, J. Chem. Soc. Dalton Trans. (1990) 413; (b) S.M. Bradley, R.A. Kydd, R. Yamdagni, Magn. Reson. Chem. 28 (1990).
[6] P. Brown, R.N. Sylva, G.E. Batley, J. Chem. Soc. Dalton Trans. (1990) 1968.
[7] C.F. Baes, R.E. Mesmer, The Hydrolysis of Cations, Wiley, New York, 1976, 152 pp.
[8] S. Hannane, F. Bertin, J. Bouix, Etude de l'hydrolyse de Zr(IV) par spectrometrie Raman et RMN du proton, Bull. Soc. Chim. Fr. (1990) 50.
[9] P. Gans, A. Sabatini, A. Vacca, J. Chem. Soc. Dalton Trans. (1985) 1195; (b) M-Meloun, J. Havel, E. Högfeldt, Computation of Solution Equilibria: A Guide to Methods in Potentiometry, Extraction and Spectrophotometry, Ellis Horwood, England, 1988.
[10] C.E. Ramos-Galván, J.M. Domínguez, G. Sandoval-Robles, A. Castillo-Mares, N. Nava-Entzana, Mat. Res. Soc. Symp. Proc., San Francisco, USA, 431, 1996, pp. 15–20.
[11] O. Ohman, W. Forsling, Acta Chem. Scand. A35 (1981) 795.
[12] J.C. Botello, MSc Thesis., UAM-I, Mexico, 1996.
[13] J.R. Mc Cauley, U.S. Patent 4, 952, 544 (1990).
[14] A. Montoya, J.M. Dominguez, A. Gomez, I. Schifter, Synthesis and properties of new catalysts: Utillization of novel materials components and synthetic techniques, in: E.C. Corcoran Jr., M.J. Ledoux (Eds.), MRS Proc. 1990 Fall Meet, Boston, Mass. USA, 1990, 93 pp.
[15] Shabtai, Massoth, Tokarz, Tasai and McCauley, Proc. 8th Int. Congr. on Catalysis, 2–6 July, 1984, Vol. IV, pp. 735–745.